Measurement xxx (xxxx) xxx–xxx

Contents lists available at ScienceDirect

Measurement

journal homepage: www.elsevier.com/locate/measurement

Development of an efficient and thermally controlled Raman system for fast and safe molecular characterization of paint layers

Andrea Azelio Mencaglia, Iacopo Osticioli, Salvatore Siano*

Istituto di Fisica Applicata "N. Carrara" – Consiglio Nazionale delle Ricerche, Via Madonna del Piano 10, 50019 Sesto Fiorentino, Italy

ARTICLE INFO

Keywords:
Raman spectroscopy
Pigment characterization
Temperature control
Painting
Archaeometry

ABSTRACT

An innovative high efficiency Raman system (exc. wav. 1064 nm) for safe molecular characterization of paint layers and other photosensitive materials has been developed and successfully tested. It was equipped with a novel optical probe, which has been designed and built in order to perform Raman scattering measurements on a relatively large spot at laser intensities lower than the typical ones of the commercial instruments. Original optical solutions were implemented in order to achieve such an improved efficiency. Furthermore, the instrument was also equipped with an active thermal control line allowing to prevent alterations of the material under study and to optimize the measurement cycles by means of suitable modulations of the laser power. Comparative tests using the novel analytical tool and an alternative setup based on a commercial Raman probe were carried out on a set of pure pigments and oil paint layers, which allowed assessing the significantly higher efficiency and reliability of the former with respect to the latter.

1. Introduction

Along the last two decades, the application of Raman spectroscopy in archaeometry and conservation of cultural heritage, as well as in other fields, has undergone significant technological and applicative advances [1]. Nowadays, this vibrational technique is becoming the most used approach for the molecular identification of pigments, binders, ceramics, and other, as well as for recognizing alteration materials and performing technological studies of a variety of artefacts, in combination with other techniques within multidisciplinary approaches (see for example [2]). Furthermore, Raman spectroscopy has also been exploited for characterizing the effectiveness of conservation treatments, such as those based on laser ablation [3]. This widespread use has been mainly favoured by the significant technological advances of the solid state lasers and optical components, along with the miniaturisation of the detectors, associated electronics, fiber coupled spectrometers, and personal computers. Such technological trends have allowed significant size and cost reductions of the analytical instruments and the development of portable devices [4,5] with spectral resolution and signal to noise ratio not far from those of the laboratory instruments. This explains the increased number of works in the recent years using homemade portable Raman setups [6–9] with special-shape probes [10] or remotely operating [11,12]. Recently, mobile instruments combining multiple spectroscopic techniques in the same system have been introduced [13–15] including for example also devices for planetary missions [16,17].

Raman spectroscopy is usually referred to as a non-destructive technique although such a safe condition can be achieved only through careful optimization of the irradiation parameters, or more often by operating at relatively low intensities. However, when the measurement time needs to be reduced in order to make practicable consecutive measurements of paint layers, organic fibers, plastics, and other, the achievement of non-destructive measurement conditions can be rather challenging because of the high photosensitivity and low critical thresholds of these materials. The excitation wavelength of 1064 nm is often preferable because of the strong fluorescence of organic materials at lower wavelengths (ex. 785 nm or lower). Anyway, because of the high intensities usually needed, the mentioned materials can easily undergo photothermal/chemical damage, such as discoloration, redox reactions, and material removal, with unacceptable visible alterations of the artefact under analysis. Furthermore, the operative conditions can become very critical whenever highly absorbing endogenous and/or exogenous materials are irradiated. Such an injury risk also represents a severe obstacle to the repeatability and reliability of the measurements and then to the possibility to implement automated compositional mapping and line-scanning Raman imaging.

In the present work, the development and comparative testing of an innovative portable Raman system (exc. wav. 1064 nm) is reported. The instrument was equipped with an optical setup allowing operating with a relatively large laser spot along with automated energy release to the

* Corresponding author.
E-mail address: S.Siano@ifac.cnr.it (S. Siano).

https://doi.org/10.1016/j.measurement.2017.11.056
Received 19 March 2017; Received in revised form 24 November 2017; Accepted 27 November 2017

target driven by an online temperature monitoring. The basic idea, working principle, and technical details of the latter were recently reported [18,19]. Besides the improvement of the whole system, here, we focus on a set of specific technical solutions and on extensive comparison carried out on pigments and paint layers with an alternative setup using a commercial Raman probe. The results achieved show the significant advantages in terms of safety and efficiency the novel analytical system, in view of molecular mapping of paintings [20–22], polychrome stones, and other.

2. Technology and methods

The novel Raman system (system A in the following) including excitation source, probe, thermal control line, spectrometer, fiber coupling, and software was designed and built according to the following component concept design: laser source with analogic power control; reflective optics with a high numerical aperture for efficient collection of the scattered radiation; laser power feedback loop for preventing material alteration based on the continuous measurement of the temperature of the irradiated spot; precise focusing and visual monitoring using LED aiming beams and a USB endoscope camera; thermal stabilization of the IR spectrometer in order to reduce the fluctuation of the background; optimization of the optical coupling between the reflective collector and the spectrometer using a suitable fiber bundle; driver and applicative software allowing for full control of the operating conditions, data acquisition, management, and display.

In Fig. 1, a detailed schematic setup of the novel probe including the described components is displayed. As shown, the DP Nd:YAG (1064 nm, 500 mW) laser was coupled to a hard clad silica (HCS) optical fiber (OF), 200/230 μm core/clad; the fiber output was imaged onto the sample (2.25× magnification) by means of an aspheric lens, L_1 (f = 18.75 mm). A 10 nm wide bandpass filter, BP, centered at 1064 nm was placed after the lens L_1 in order to cut-off the Raman scattering contribution of the fiber. The optical collector was devised using a pair of off-axis, 90°, parabolic mirrors, ½ inch diameter. The primary one, M_1, which was drilled in order to let the laser beam pass through, had a focal length of 15 mm (NA: 0.41) while that of the secondary one, M_2,

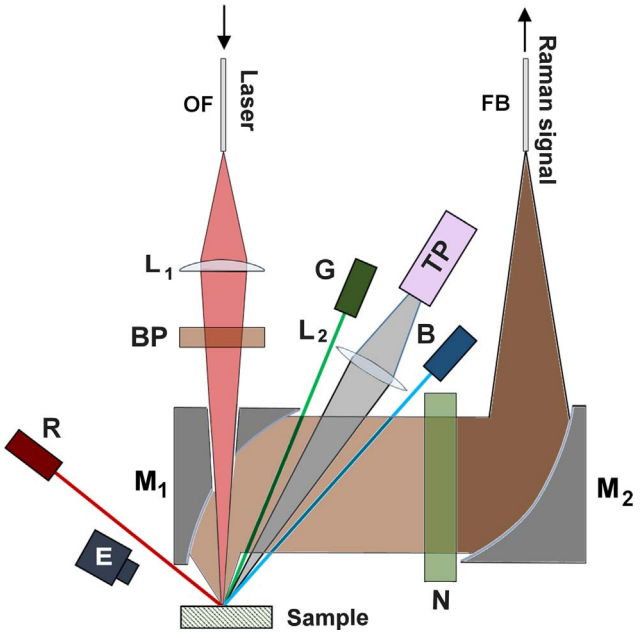

Fig. 1. Schematic set up of the novel probe implemented in the Raman system A. $L_{1\text{-}2}$: lenses. $M_{1\text{-}2}$: 90° off-axis parabolic mirrors. BP and N: bandpass and notch filter, respectively. TP: thermopile. R, G, B: red green and blue LEDs, respectively. E: endoscope camera. (For interpretation of the references to colour in this figure legend, the reader is referred to the web version of this article.)

was 25.4 mm. The latter was selected in order to better match the numerical aperture of the fiber. The optimization of the coupling to the spectrometer was achieved through comparative tests using different fibers and bundles. The best results were provided by a fiber bundle with seven fibers (∅ 105/125 μm core/clad, NA = 0.22), packed circularly at the input tip (collector side) and linearly at the output one (spectrometer side), which was aligned along the direction of entrance slit. The notch filter (N), centred @ 1064 nm, 44 nm-wide blocking window (OD > 6) for rejecting the elastic scattering component, was placed between the two mirrors. The IR spectrometer included a monochromator and a 512-pixel deep-cooled (−55 °C) InGaAs array detector (BaySpec Inc., CA, USA), allowing to cover the spectral range between 165 and 1825 cm^{-1} with a resolution of 8 cm^{-1}. As anticipated above, the spectrometer was thermally stabilized using Peltier cells, suitable casing, fan, and heat sink components.

The thermopile sensor (TP) was calibrated according to a corrected blackbody emission formula and the direct measurement of the emissivity of the target in order to provide the temperature evolution $T(t)$ at the irradiated area, which was imaged on the sensor by means of the ZnSe lens, L_2 (see [18] for further details). $T(t)$ was used as input observable of the power control, $P(t)$, with Proportional-Integral (PI) feedback:

$$P(t) = \begin{cases} B{\cdot}\Delta T(t)^{\frac{1}{5}}\tanh\left(\frac{t}{\tau}\right) + C{\cdot}\int_0^t \Delta T(t')^{\frac{1}{5}}dt', & \text{if } \Delta T(t) > 0 \\ P_{min}, & \text{if } \Delta T(t) \leqslant 0 \end{cases} \quad (1)$$

where $\Delta T(t) = T_{set} - T(t)$, B, C and τ are adjustable parameters, T_{set} is the expected temperature set by the operator, while P_{min} was set at 20 mW (arbitrary value selected in order to avoid the switch-off of the laser when deep power modulations were induced by rapid temperature rises).

The suitable selection of the B, C and τ parameters allowed optimizing the laser energy release to the target in order to avoid undesired overheating and alteration of the sample under analysis. In some details τ = 0.7 s guaranteed a gradual power increase during the onset phase, which was needed in order to avoid too high thermal gradients within the response time of the thermopile, TP (1.3 s). B can assume values ranging between 2.8 and 28 $mW°C^{-1/5}$, while C ranges between $8.4{\cdot}10^{-3}$ and $42{\cdot}10^{-3}$ $mW°C^{-1/5}s^{-1}$.

Three light beams (less than 1 mm diameter) were projected onto the sample surface by three LEDs (red, blue and green: R, G, B in Fig. 1), coupled to steel hollow needles 25 mm length, in such a way they overlapped at the focal spot of the system. These aiming beams along with an USB endoscope camera (E in Fig. 1) allowed controlling easily the correct positioning of the sample before the spectrum collection.

The performances of the Raman system A, just described, were compared with those of an alternative setup (system B) built using the same laser excitation source and spectrometer as those of the system A and the commercial probe schematized in Fig. 2. In this second case, the scattered light was collected and collimated by the same lens, L_2 (NA = 0.4), used for focusing the laser beam (focal spot diameter of 105 μm). It was then extracted from the incidence optical axis by means of a dichroic mirror (DM), bent using a flat mirror (M), filtered (N), coupled to the optical fiber (200 μm core diameter), and eventually sent to the spectrometer.

The comparison between the two systems was carried out by considering the following exposure-normalised detection efficiency parameter:

$$\varepsilon = \frac{I_R}{\int_0^{t_L} I_L(t)dt} = \frac{I_R}{F_{tot}} = \left[\frac{counts}{J/cm^2}\right], \quad (2)$$

where I_R is the peak intensity of the Raman band (after baseline subtraction) selected for comparison, I_L the laser intensity, t_L the irradiation time, and F_{tot} the total fluence of radiant exposure at the focal laser spot. Alternatively, the detection performance can be compared by